

Improved Cine Cardiovascular Magnetic Resonance Using Clariscan™ (NC100150 Injection)

Nicholas H. Bunce,¹ James C. C. Moon,¹
Nicholas G. Bellenger,¹ Jennifer Keegan,¹
Frank Grothues,¹ Jane A. McCrohon,¹
Jane M. Francis,¹ Gillian C. Smith,¹
Elisabeth D. Burman,¹ David N. Firmin,¹
Volker W. Hoffmann,² and Dudley J. Pennell¹

¹Cardiovascular Magnetic Resonance Unit, Royal Brompton Hospital,
London, United Kingdom

²Nycomed Amersham, Munich, Germany

ABSTRACT

We evaluated the use of Clariscan™ 0.75, 2, and 5 mg Fe/kg body weight in six patients to determine optimal dosing for short repetition time cine imaging. Breathhold cine images were acquired in the vertical and horizontal long axes and the short axis. Blood-pool signal-to-noise ratio increased significantly in all planes ($p < 0.01$) but was least marked in the short axis. Myocardial signal-to-noise ratio increased by a lesser amount ($p < 0.05$). Myocardial to blood-pool signal-difference-to-noise ratio improved significantly in the long axes ($p < 0.05$) and was greatest at 2 mg Fe/kg body weight, but changes in the short axis were minor. With the 5-mg Fe/kg body weight dose, the response was reduced or reversed due to T2 effects. Visual assessment improved in all planes ($p < 0.05$) and was optimal at 2 mg Fe/kg body weight. In conclusion, Clariscan improves short repetition time cardiac breathhold cine imaging, particularly in the long axis planes, with an optimal dose of 2 mg Fe/kg body weight.*

Key Words: Cardiac function; Clariscan™; Short TR breathhold cine imaging

Address correspondence and reprint requests to Nicholas H. Bunce.

INTRODUCTION

Cardiovascular magnetic resonance is an increasingly useful tool for the accurate assessment of cardiac function and wall motion abnormalities in patients with cardiac disease (1–4). It is possible to acquire good quality breathhold gradient echo (fast low angle shot [FLASH]) cine images in healthy subjects with normal cardiac function and blood flow who can cooperate with breathhold instructions (5). However, in patients with impaired ventricular function, blood flow can be slow, leading to a reduction in the quality of the images, which is exacerbated by difficulties in breathholding due to orthopnea (6). These problems can interfere with the accurate measurement of ventricular volume and wall motion by reducing myocardium to blood-pool contrast, especially in the apex and around the papillary muscles. In addition, the increasing requirement for greater temporal resolution in stress studies during tachycardia (7,8) and the possibility of developing a three-dimensional volumetric technique (9) have led to cine imaging with short repetition time (TR), which also exacerbates the problem.

One method to improve the blood-pool to myocardium contrast is to give a T1 shortening agent. Extravascular gadolinium contrast agents have been shown to be effective (10), but the improvement in cine quality is relatively modest and short lived, and a more ideal T1 shortening agent should be intravascular with a longer duration of action. Clariscan™ (feruglose; Nycomed Amersham Imaging, Oslo, Norway) is an ultras-small superparamagnetic iron oxide that remains in the intravascular space. In normal subjects it has been shown to be safe (11) and improves image quality and blood-pool to myocardium contrast (12). Clariscan has a prolonged half-life of greater than 2 hr and has been shown to have potential application for perfusion (13), function (12), and coro-

nary imaging (11). In this study we investigate the effects of cumulative doses of Clariscan on breathhold short TR gradient echo cine imaging in patients with impaired systolic ventricular function as part of a multicenter phase 2 study.

MATERIALS AND METHODS

Six patients with documented cardiac disease and a mean ejection fraction of 36% (range, 22–56%; Table 1) determined by radionuclide ventriculography were studied using a 1.5-T Edge scanner (Picker, Cleveland, OH). The patients were all clinically stable and were recruited from a cardiac outpatient clinic. All subjects gave informed consent, and the study was approved by the Hospital Ethics Committee. Safety follow-up was continued for 72 hr after dosing.

Using initial scout images for orientation, baseline breathhold FLASH cine images were acquired in the vertical long axis (VLA), horizontal long axis (HLA), and a mid-ventricular short axis (SA) of the left ventricle. Then Clariscan 0.75 mg Fe/kg body weight was administered as a slow bolus via a cannula in the antecubital fossa. After allowing 2 min for Clariscan to reach a steady-state concentration within the blood, the breathhold cine scans were repeated. After 20 and 40 min, further boluses were given to a total dosage of 2 mg and 5 mg Fe/kg body weight, and the scans were repeated at each dose increment. All images were acquired with electrocardiographic gating, and the breathhold duration was adjusted according to the patient's heart rate and ability to breathhold. For each individual patient, the breathhold duration was kept constant before and after each incremental dose.

Table 1
Patient Characteristics

Patient	Age (yr)	Sex	Ejection Fraction (%)	Electrocardiogram	Heart Rate	Clinical Diagnoses
1	59	M	22	SR	80	CABG; myocardial infarction
2	77	M	30	AF, LBBB	90	Myocardial infarction, heart failure
3	66	M	23	SR, LBBB	72	Aortic valve replacement, heart failure
4	51	M	56	AF	80	Hypertension; cardiomyopathy
5	80	M	52	SR, LBBB	60	Aortic regurgitation
6	66	M	34	SR	75	CABG, mitral regurgitation

SR, sinus rhythm; AF, atrial fibrillation; LBBB, left bundle branch block; CABG, coronary artery bypass grafts.



Contrast Agent

Clariscan (feruglose, 30 mg Fe/ml) is an aqueous colloidal solution of nanosized superparamagnetic iron oxide particles (particle size of approximately 6 nm) with an oxidized starch coating. The preparation exerts a relatively high T1 ($r_1 = 21.8 \text{ mmol}^{-1}\text{sec}^{-1}$) and a relatively weak T2 relaxivity ($r_2 = 35.3 \text{ mmol}^{-1}\text{sec}^{-1}$) at 20 MHz, 37°C (14). Clariscan has intravascular distribution and a plasma half-life time > 2 hr.

Imaging Protocol

Imaging was performed using a breathhold segmented gradient echo FLASH sequence with a quadrature body coil. Initial coronal and transverse pilot scans were used to identify the VLA of the left ventricle, and then from this scan the HLA and then SA were positioned (Fig. 1). For each imaging plane the imaging parameters were as follows: echo time (TE) 2 msec, TR 5 msec, flip angle

35 degrees, slice thickness 8 mm, field of view 35–40 × 40 cm, matrix 128 × 256, number of excitations 1, and cine phases 12–20. The views per segment (six to eight) depended on the patients’ heart rate and ability to breathhold, and the total breathhold duration was 10–16 sec. For each patient, imaging parameters were identical before and after contrast.

Image Analysis

The images were analyzed off-line using in-house software, CMRtools (© Royal Brompton and Harefield NHS Trust). A circular region of interest (5 mm in diameter) was positioned within the septum of the HLA and SA images and the anterior wall for the VLA and the mean myocardial signal intensity obtained. For all images, blood-pool signal intensity was measured by positioning a circular region of interest (5 mm in diameter) within the blood pool. Noise was measured as the SD of the signal in a rectangular region of interest (40 × 20

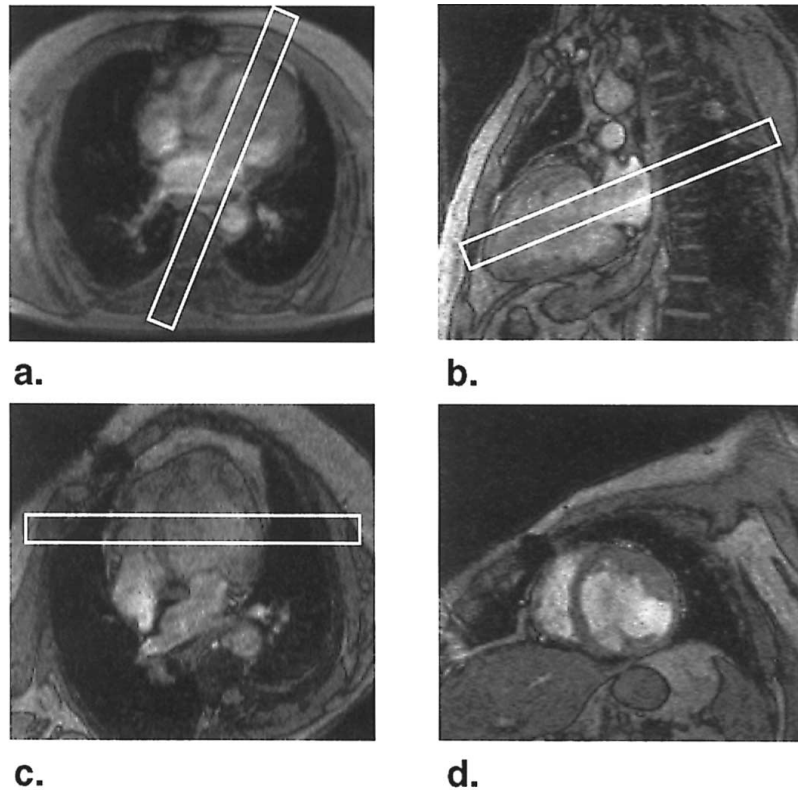


Figure 1. From an initial transverse pilot scan (a), the vertical long axis of the left ventricle can be acquired (b). From this, the horizontal long axis (c) and the short axis (d) are obtained.

mm) placed outside the phase encode artifact (12,15). For each gradient echo image (VLA, HLA, and SA), a signal-to-noise ratio was calculated for both the LV blood pool and LV myocardium, at both end-diastole and end-systole, before and after each dose of Clariscan. After each dose of Clariscan, a signal-difference-to-noise ratio (blood-pool signal minus myocardial signal divided by noise) was calculated for each image at end-diastole and end-systole (6,16).

The images were independently assessed by two experienced observers, blinded to the dose of Clariscan received for each image, using the following visual scoring system: 1, poor myocardial wall definition/blood pool obscured; 2, reasonable myocardial wall definition/some blood-pool blurring; 3, good myocardial wall definition/minor blood-pool blurring; 4, very good myocardial wall definition/no blood-pool blurring; 5, excellent wall definition/no blood-pool blurring. The average score from the two observers was used for the analysis. Although there was some variation in the imaging parameters between patients (field of view, views per segment, number of cine phases acquired), the parameters were held constant for any individual patient, and the differences in signal-to-noise ratio and contrast and image quality could therefore be attributed to the contrast agent alone.

Statistical analysis was performed using SPSS v9.0 (SPSS Inc., Chicago, IL). Because of the small number of subjects studied, it was not possible to determine normality of the data and so nonparametric methods of analysis were used. The Friedman test was used to compare myocardial signal-to-noise ratio, blood-pool signal-to-noise ratio, signal difference-to-noise-ratio, and visual scores before contrast and with each dose of Clariscan. If a significant difference ($p < 0.05$) was obtained, a Wilcoxon signed rank test was performed between the pre-contrast result and each separate dose of Clariscan.

RESULTS

There were no serious adverse reactions to Clariscan. In the six subjects studied there were no significant differences in heart rate, systolic or diastolic blood pressure, or 12-lead electrocardiograms compared with baseline at any of the three doses of Clariscan or over the follow-up period of 72 hr.

For all three imaging planes (HLA, VLA and SA), Clariscan significantly ($p < 0.01$) increased the mean blood-pool signal-to-noise ratio compared with baseline in both diastole and systole at all dose levels, with the

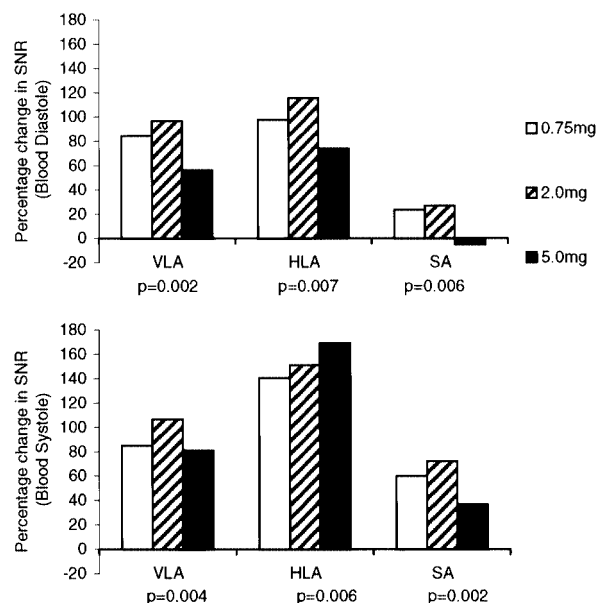


Figure 2. The percentage change in blood signal-to-noise ratio (SNR) after each dose of Clariscan™ compared with baseline is shown in diastole (top) and systole (bottom) for each plane. The greatest increases are seen in the VLA and HLA planes. The percentage change in the SA plane is smaller and is below precontrast level at the 5-mg dose in diastole. The p values shown refer to the Friedman test comparing baseline with all dose groups for the percentage change in SNR.

exception of the SA 5-mg Fe/kg body weight dose (Fig. 2). The increase in signal-to-noise ratio was greatest in the long-axis planes (range, 56–169%) compared with the short axis (range, -5% to 72%). Compared with the unenhanced scan, myocardial signal-to-noise ratio also increased significantly (15–61%, $p < 0.05$) and at all dose levels in the VLA and SA, but the increase was of a lower magnitude than for the blood pool (Fig. 3). In the HLA, there was a slightly more variable response, and although increases in signal-to-noise ratio were seen, these just failed to reach statistical significance with the small sample size in this study. Trends between diastole and systole and between long- and short-axis planes were less pronounced than for the blood pool.

The LV blood-pool to myocardium signal difference-to-noise-ratio for each dose of Clariscan at end-diastole and end-systole for each image plane is shown in Fig. 4. In the VLA, in systole, there was a significant increase in the signal difference-to-noise-ratio with each dose of Clariscan, but in diastole only the 0.75- and 2-mg Fe/kg body weight doses showed improvement. In the HLA in both diastole and systole, there was a significant increase

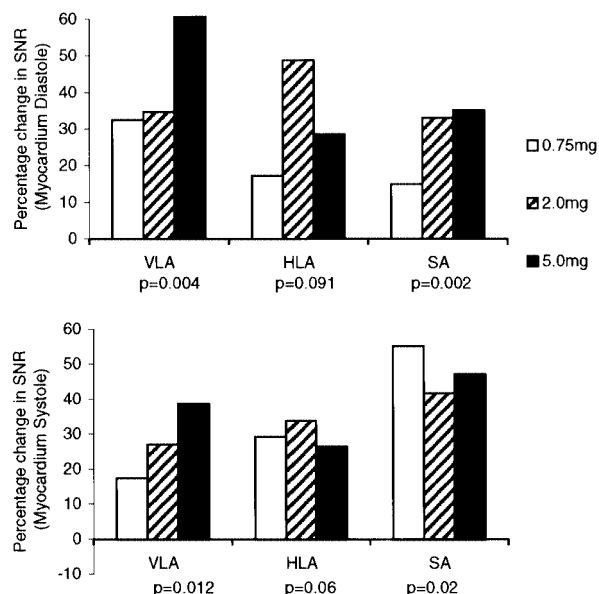


Figure 3. The percentage change in myocardial signal-to-noise ratio (SNR) in both diastole (top) and systole (bottom) compared with baseline is shown for each dose of Clariscan™. The changes in the VLA and SA were significant, and in the HLA were borderline significant. Note that the vertical scale of both graphs is greater than that shown in Fig. 2, indicating that the signal increase in the blood pool is two to three times greater than in the myocardium. The *p* values shown refer to the Friedman test comparing baseline with all dose groups for the percentage change in SNR.

in the signal difference-to-noise-ratio with each dose of Clariscan. In the SA, the diastolic signal difference-to-noise-ratio before and after Clariscan was unchanged for the 0.75- and 2-mg Fe/kg doses compared with pre-contrast, and at 5 mg Fe/kg the signal difference-to-noise-ratio was reduced. At end-systole, only the 2-mg Fe/kg dose showed a significant improvement in signal difference-to-noise-ratio.

The results for the visual analysis are displayed in Table 2 for both diastolic and systolic images. The visual analysis scores after Clariscan were significantly better ($p < 0.05$) for all doses in the VLA and HLA planes except for the 5-mg dose in the VLA plane at end-diastole. In the SA plane, in diastole, there was no significant improvement after the 0.75- and 2-mg Fe/kg body weight doses and a significant deterioration after the top dose. In the SA plane, in systole, only the 2-mg Fe/kg dose showed a significant improvement in image quality. Optimal quality scores were found in all planes at the 2-mg Fe/kg dose. Sample images are displayed in Fig. 5 for

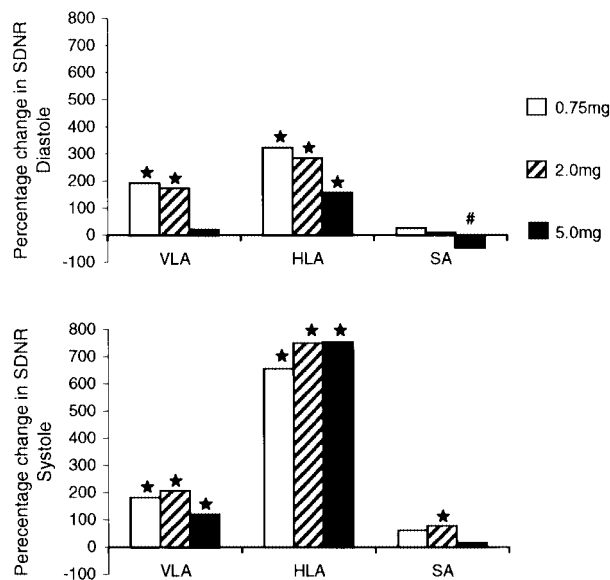


Figure 4. The percentage change in signal difference-to-noise ratio (SDNR) in both systole (top) and diastole (bottom) compared with baseline is shown for each dose of Clariscan™. For the VLA and HLA significant improvements are seen with optimal improvements at 2 mg Fe/kg body weight. For the SA there are no improvements after Clariscan™, and the 5-mg dose shows a significant worsening of SDNR. * $p < 0.05$ for improvement, # $p < 0.05$ for worsening of SDNR versus baseline.

all three slices before and after Clariscan 2 mg Fe/kg body weight.

DISCUSSION

Breathhold gradient echo cine images are commonly used in cardiovascular magnetic resonance for the assessment of ventricular function. Quantitative analysis of the cine images forms the basis of left and right ventricular ejection fraction determination (17) used in patients with heart failure and in patients with regurgitant cardiac valves. In addition, a qualitative assessment of myocardial wall motion abnormalities in myocardial hibernation studies, cardiomyopathies, and myocardial ischaemia is an important part of the clinical diagnosis (18,19). Both approaches require good myocardial to blood-pool border definition. However, many of these patients will have impaired ventricular function, with abnormally slow-flowing blood leading to reduced inflow enhancement and poor myocardium to blood-pool contrast. The situation is further exacerbated by short TR imaging required for high temporal resolution studies to enable the acquisition

Table 2
Visual Scores

Mean Visual Score	Diastole			Systole		
	VLA	HLA	SA	VLA	HLA	SA
Precontrast	1.8	1.3	2.9	1.3	1.0	2.1
0.75	3.3*	3.3*	3.3	2.8*	2.8*	2.6
2.0	4.1*	3.9*	3.2	3.9*	3.9*	3.2*
5.0	2.8	3.5*	2.1†	3.3*	3.8*	2.9
Friedman test	0.006	0.002	0.005	0.001	0.001	0.014

The mean visual score for each image plane (VLA, HLA, SA) and at each dose is shown. The optimal score occurred with the 2-mg Fe/kg body weight dose in all planes.

* $p < 0.05$ for improvement.

† $p < 0.05$ for worsening of cine score vs. baseline, Wilcoxon signed rank test.

of an adequate number of cine phases through the cardiac cycle during dobutamine stress testing when heart rates of 120–140 beats/min are typical. The performance of three-dimensional volumetry causes similar problems. Although the blood-pool/myocardium contrast may be improved by implementing a short TE/short TR steady-state free precession type sequence (20), these have not yet been validated in human LV studies. An alternative method is to give an intravascular contrast agent that reduces the T1 of blood compared with myocardium and allows non-first-pass imaging with a segmented FLASH sequence.

In an earlier study, we demonstrated that Clariscan could improve cine images in healthy volunteers with normal cardiac function and blood flow (12). However, in that study although Clariscan improved gradient echo and spin echo images, a dose–response relationship for Clariscan was not obtained and the effects in the long and short axes of the heart were not assessed. In this study, incremental doses of Clariscan were assessed up to a total dose of 5 mg Fe/kg body weight. The long half-life of this agent makes it unlikely that the effects observed would differ substantially from those observed after the administration of a single dose of the same magnitude.

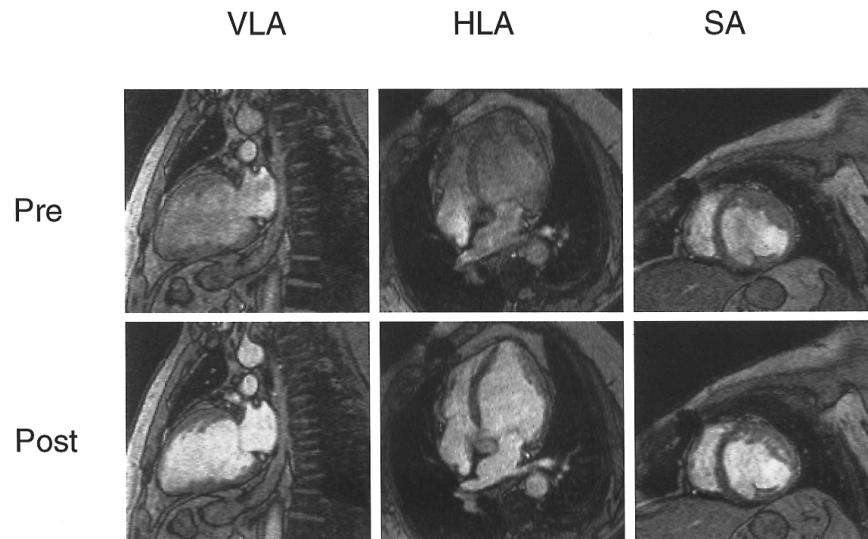


Figure 5. Example of the improved image quality of the VLA, HLA, and SA planes (Clariscan™ 2 mg Fe/kg). Top: precontrast; bottom: postcontrast.

In this study, Clariscan produced a marked increase in the LV blood-pool signal-to-noise ratio in all planes and doses used (except for 5 mg Fe/kg in the diastolic SA view). This was most striking in the long-axis planes where blood flow is known to be more in-plane compared with the short axis, and signal-to-noise ratio increases up to 168% were found. In general, the signal-to-noise ratio increased to a plateau with the second dose of Clariscan (2 mg Fe/kg) and then declined for the 5-mg Fe/kg dose. There was also an increase in myocardial signal-to-noise ratio across all three doses of Clariscan, but this rise was of generally lower magnitude than for the blood pool. Overall, the LV blood-pool to myocardial signal difference-to-noise-ratio, which is a measure of the contrast between LV blood and myocardium independent of display, showed significant improvements, especially with the lower doses. For both long-axis planes, there was a large and significant increase in the signal difference-to-noise-ratio in both diastole and systole for the 0.75- and 2-mg Fe/kg doses compared with the unenhanced scan. This was also demonstrated with the visual analysis scores (Table 2). Using Clariscan in two cases, it was possible to clearly delineate LV apical aneurysms that could not be seen before contrast. There appeared to be no benefit from increasing the Clariscan dose to 5 mg Fe/kg, and in most cases there was a deterioration in both signal difference-to-noise ratio and image quality. This may be due to the T2* effects of Clariscan that have been observed in previous studies with higher doses (13,21). This was observed in our study despite using a sequence with a short TE designed to minimize the T2* effects. In the SA plane, the blood-pool signal difference-to-noise ratio was high at baseline due to the through-plane blood inflow, and therefore the effects of Clariscan in this plane were not as large as in the VLA and HLA, but a significant improvement at 2 mg Fe/kg was seen in systole. On visual analysis scores, Clariscan produced nonsignificant improvements but reduced the blurring of borders seen in patients with slow blood flow.

CONCLUSION

In this study of patients with abnormal systolic ventricular function, Clariscan significantly increased blood-pool signal-to-noise ratio and blood-pool to myocardium signal difference-to-noise ratio. It also improved subjective image quality and delineation of the LV endocardial-blood-pool border. The optimal dose at 1.5 T was 2 mg Fe/kg body weight. There was no further improvement at higher doses, probably due to T2* effects. It is

possible that these improvements might prove useful for dobutamine stress cine studies and improve automated border detection software for the quantification of LV volumes. Three-dimensional LV volume studies might also be developed to improve slice to slice registration that can be problematic with the multiple two-dimensional breathhold approach with variable diaphragm positions between breathholds, unless navigator techniques are used (22). The drug was safe, easy to use, and allowed imaging for up to 60 min after intravenous injection.

ACKNOWLEDGMENTS

Clariscan™ was provided by Nycomed Amersham. This study was supported by CODA the heart charity and the Wellcome Trust, who have no financial interest in the commercialization of this product.

REFERENCES

1. Bellenger, N.G.; Francis, J.M.; Davies, C.L.; Coats, A.; Pennell, D.J. Establishment and Performance of a Magnetic Resonance Cardiac Function Clinic. *J. Cardiovasc. Magn. Reson.* **2000**, *2*, 15–22.
2. Bellenger, N.G.; Marcus, N.J.; Grieve, L.; Yacoub, M.H.; Banner, N.R.; Pennell, D.J. Left Ventricular Function and Mass After Orthotopic Heart Transplantation: A Comparison of Cardiovascular Magnetic Resonance With Echocardiography. *J. Heart Lung Transplant.* **2000**, *19*, 444–452.
3. Bellenger, N.G.; Marcus, N.; Davies, C.L.; Coats, A.; Lahiri, A.; Cleland, J.G.F.; Pennell, D.J., on behalf of the CHRISTMAS Steering Committee and Investigators. Comparison of Left Ventricular Ejection Fraction and Volumes in Heart Failure by Two-Dimensional Echocardiography, Radionuclide Ventriculography and Cardiovascular Magnetic Resonance: Are They Interchangeable? *Eur Heart J.* **2000**, *21*, 1387–1396.
4. Bellenger N.G.; Davies, L.C.; Francis, J.M.; Coats, A.J.S.; Pennell, D.J. Reduction in Sample Size for Studies of Remodeling in Heart Failure by the Use of Cardiovascular Magnetic Resonance. *J. Cardiovasc. Magn. Res.* **2000**, *4*, 271–278.
5. Semelka, R.C.; Tomei, E.; Wagner, S.; Mayo, J.; Kondo, C.; Suzuki, J.; Caputo, G.R.; Higgins, C.B. Normal Left Ventricular Dimensions and Function: Interstudy Reproducibility of Measurements with Cine MR Imaging. *Radiology* **1990**; *174*, 763–768.
6. Taylor, A.M.; Keegan, J.; Jhooti, P.; Gatehouse, P.D.; Firmin, D.N.; Pennell, D.J. Differences Between Normal Subjects and Patients with Coronary Artery Disease for Three Different MR Coronary Angiography Respiratory



- Suppression Techniques. *J. Magn. Reson. Imaging* **1999**; *9*, 786–793.
7. Pennell, D.J.; Underwood, S.R.; Manzara, C.C.; Ell, P.J.; Swanton, R.H.; Walker, J.M.; Longmore, D.B. Magnetic Resonance Imaging During Dobutamine Stress in Coronary Artery Disease. *Am. J. Cardiol.* **1992**, *70*, 34–40.
 8. Pennell, D.J.; Firmin, D.N.; Burger, P.; Yang, G.Z.; Manzara, C.C.; Ell, P.J.; Swanton, R.H.; Walker, J.M.; Underwood, S.R.; Longmore, D.B. Assessment of Magnetic Resonance Velocity Mapping of Global Ventricular Function During Dobutamine Infusion in Coronary Artery Disease. *Br. Heart J.* **1995**, *74*, 163–170.
 9. Amano, Y.; Herfkens, R.J.; Shifrin, R.Y.; Alley, M.T.; Pelc, N.J. Three-Dimensional Cardiac Cine Magnetic Resonance Imaging with an Ultrasmall Superparamagnetic Iron Oxide Blood Pool Agent. *J. Magn. Reson. Imaging* **2000**, *11*, 81–86.
 10. Pennell, D.J.; Underwood, S.R.; Longmore, D.B. Improved Cine Magnetic Resonance Imaging of the Left Ventricular Wall Motion Using Gadopentetate-Dimeglumine. *J. Magn. Reson. Imaging*, **1993**, *3*, 13–19.
 11. Taylor, A.M.; Panting, J.R.; Keegan, J.; Gatehouse, P.D.; Amin, D.; Jhooti, P.; Yang, G.Z.; McGill, S.; Burman, E.D.; Francis, J.M.; Firmin, D.N.; Pennell, D.J. Safety and Preliminary Findings with the Intravascular Contrast Agent NC100150 Injection for MR Coronary Angiography. *J. Magn. Reson. Imaging* **1999**, *9*, 220–227.
 12. Taylor, A.M.; Panting, J.R.; Keegan, J.; Gatehouse, P.D.; Jhooti, P.; Yang, G.Z.; McGill, S.; Francis, J.M.; Burman, E.D.; Firmin, D.N.; Pennell, D.J. Use of the Intravascular Contrast Agent NC100150 Injection in Spin Echo and Gradient Echo Imaging of the Heart. *J. Cardiovasc. Magn. Reson.* **1999**, *1*, 23–32.
 13. Panting, J.R.; Taylor, A.M.; Gatehouse, P.D.; Keegan, J.; Yang, G.Z.; McGill, S.; Francis, J.M.; Burman, E.D.; Firmin, D.N.; Pennell, D.J. First-Pass Myocardial Perfusion Imaging and Equilibrium Signal Changes Using the Intravascular Contrast Agent NC100150 Injection. *J. Magn. Reson. Imaging* **1999**, *10*, 404–410.
 14. Kellar, K.E.; Fujii, D.K.; Gunther, W.H.; Briley-Saebo, K.; Bjornerud, A.; Spiller, M.; Koenig, S.H. NC100150 Injection. *J. Magn. Reson. Imaging* **2000**, *11*, 488–494.
 15. Kaufman, L.; Kramer, D.M.; Crooks, L.E.; Ortendahl, D.A. Measuring Signal-to-Noise Ratios in MR Imaging. *Radiology* **1989**, *173*, 265–267.
 16. Wolff, S.D.; Balaban, R.S. Assessing Contrast on MR Images. *Radiology* **1997**; *202*, 25–29.
 17. Lorenz, C.H.; Walker, E.S.; Morgan, V.L.; Klein, S.S.; Graham, T.P. Normal Human Right and Left Ventricular Mass, Systolic Function and Gender Differences by Cine Magnetic Resonance Imaging. *J. Cardiovasc. Magn. Reson.* **1999**, *1*, 7–21.
 18. Gunning, M.G.; Anagnostopoulos, C.; Knight, C.J.; Pepper, J.; Burman, E.D.; Davies, G.; Fox, K.M.; Pennell, D.J.; Ell, P.J.; Underwood, S.R. Comparison of 201Tl, 99mTc-Tetrofosmin, and Dobutamine Magnetic Resonance Imaging for Identifying Hibernating Myocardium. *Circulation* **1998**, *98*, 1869–1874.
 19. Blake, L.M.; Schneimann, M.M.; Higgins, C.B. MR Features of Arrhythmogenic Right Ventricular Dysplasia. *AJR Am. J. Roentgenol.* **1994**, *162*, 809–812.
 20. Van der Meulen, P.; Groen, J.P.; Tinus, A.M.; Bruntink, G. Fast Field Echo Imaging: An Overview and Contrast Calculations. *Magn. Reson. Imaging* **1988**, *6*, 355–368.
 21. Wilkstrom, L.J.; Johansson, L.O.; Ericsson, B.A.; Borseth, A.; Akeson, P.A.; Ahlstrom, K.H. Abdominal Vessel Enhancement with an Ultrasmall, Superparamagnetic Iron Oxide Blood Pool Agent: Evaluation of Dose and Echo Time Dependence at Difference. *Acad. Radiol.* **1999**, *6*, 292–298.
 22. Bellenger, N.G.; Gatehouse, P.D.; Rajappan, K.; Keegan, J.; Firmin, D.N.; Pennell, D.J. Left Ventricular Quantification in Heart Failure by CMR Using Prospective Respiratory Navigator Gating: Comparison with Breath-Hold Acquisition. *J. Magn. Reson. Imaging* **2000**, *11*, 411–417.

Received September 22, 2000

Accepted February 19, 2001



Request Permission or Order Reprints Instantly!

Interested in copying and sharing this article? In most cases, U.S. Copyright Law requires that you get permission from the article's rightsholder before using copyrighted content.

All information and materials found in this article, including but not limited to text, trademarks, patents, logos, graphics and images (the "Materials"), are the copyrighted works and other forms of intellectual property of Marcel Dekker, Inc., or its licensors. All rights not expressly granted are reserved.

Get permission to lawfully reproduce and distribute the Materials or order reprints quickly and painlessly. Simply click on the "Request Permission/Reprints Here" link below and follow the instructions. Visit the [U.S. Copyright Office](#) for information on Fair Use limitations of U.S. copyright law. Please refer to The Association of American Publishers' (AAP) website for guidelines on [Fair Use in the Classroom](#).

The Materials are for your personal use only and cannot be reformatted, reposted, resold or distributed by electronic means or otherwise without permission from Marcel Dekker, Inc. Marcel Dekker, Inc. grants you the limited right to display the Materials only on your personal computer or personal wireless device, and to copy and download single copies of such Materials provided that any copyright, trademark or other notice appearing on such Materials is also retained by, displayed, copied or downloaded as part of the Materials and is not removed or obscured, and provided you do not edit, modify, alter or enhance the Materials. Please refer to our [Website User Agreement](#) for more details.

[Order now!](#)

Reprints of this article can also be ordered at

<http://www.dekker.com/servlet/product/DOI/101081JCMR100108583>